HAL
open science

A high pressure oxidation study of di-n-propyl ether

Maxence Lailliau, Guillaume Dayma, Philippe Dagaut, Zeynep Serinyel

To cite this version:

Maxence Lailliau, Guillaume Dayma, Philippe Dagaut, Zeynep Serinyel. A high pressure oxidation study of di-n-propyl ether. Fuel, 2020, 263, pp.116554. 10.1016/j.fuel.2019.116554 . hal-02934437

HAL Id: hal-02934437

https://hal.science/hal-02934437v1

Submitted on 9 Sep 2020

HAL is a multi-disciplinary open access archive for the deposit and dissemination of scientific research documents, whether they are published or not. The documents may come from teaching and research institutions in France or abroad, or from public or private research centers.

L'archive ouverte pluridisciplinaire **HAL**, est destinée au dépôt et à la diffusion de documents scientifiques de niveau recherche, publiés ou non, émanant des établissements d'enseignement et de recherche français ou étrangers, des laboratoires publics ou privés.

Copyright

A high pressure oxidation study of di-n-propyl ether

Zeynep Serinyel*[1,2], Maxence Lailliau[1,2], Guillaume Dayma[1,2], and Philippe Dagaut[2]

[1] Collegium Sciences et Techniques, Université d'Orléans, rue de Chartres, 45100 Orléans

[2] CNRS–ICARE, 1C avenue de la Recherche Scientifique, 45071 Orléans cedex 2

*Corresponding author:

Zeynep Serinyel, PhD

CNRS–ICARE, Institut de Combustion, Aérothermique, Réactivité et Environnement

1C Avenue de la Recherche Scientifique

45071 Orléans Cedex 2, France

Tel : +33 (0)2 38 25 77 77

zeynep.serinyel@cnrs-orleans.fr

Abstract

The oxidation of di-n-propyl-ether (DPE), was studied in a jet-stirred reactor. Fuel-lean, stoichiometric and fuel-rich mixtures (φ = 0.5–4) were oxidized at a constant fuel mole fraction of 1000 ppm, at temperatures ranging from 470 to 1160 K, at 10 atm, and constant residence time of 700 ms. The mole fraction profiles were obtained through sonic probe sampling and gas chromatography and Fourier transform infrared spectrometry analyses. As was the case in our previous studies on ethers (diethyl ether and di-n-butyl ether), the carbon neighboring the ether group was found to be the most favorable site for H-abstraction reactions and the chemistry of the corresponding fuel radical drives the overall reactivity. The fuel concentration profiles indicated strong low-temperature chemistry. A kinetic sub-mechanism is developed based on rules similar to those for the two symmetric ethers previously investigated (DEE and DBE). The proposed mechanism shows good performances in representing the present experimental data, nevertheless, more data such as atmospheric pressure speciation will be needed in order to better interpret the kinetic behavior of DPE.

Introduction

Given the strict emission regulations for automotive sector and environmental concerns, there has recently been a growing need to find alternative feedstocks for the next generation biofuels. These include di-n-butyl ether (DBE, C_4H_9–O–C_4H_9), diethyl ether (DEE, C_2H_5–O–C_2H_5), and dimethyl ether (DME, CH_3–O–CH_3) among many other families of oxygenated molecules. DBE can be produced from lignocellulosic source, while DEE can be produced from bioethanol by dehydration. Very recently, DBE and DEE received a lot of interest. They were studied in different laboratory set-ups, in terms of oxidation, pyrolysis, ignition delays, laminar flame speeds, and laminar flame structure [1-8].

Our team has recently studied the oxidation of DBE and DEE in jet-stirred reactor [6, 9]. An unusual oxidation behavior showing double-NTC region was observed with DBE, which was not the case with DEE under the same conditions, the latter having shown conventional low-temperature reactivity. Di-n-propyl ether (DPE, C_3H_7–O–C_3H_7), on the other hand, is not considered a potential biofuel and has not been studied in combustion. However, in terms of carbon number, this symmetric ether is between DEE and DBE. It is therefore of fundamental interest to study its oxidation behavior. The structures of these ethers are shown in figure 1.

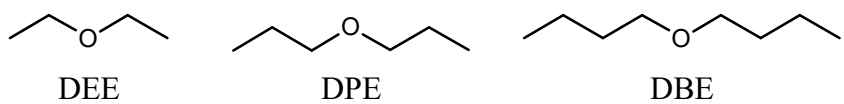

Figure 1. Structures of diethyl, di-n-propyl and di-n-butyl ethers

Oxidation of DPE, is therefore studied in the same experimental conditions as DEE and DBE, 10 atm, between 470 to 1160 K. A kinetic sub-model is developed for this fuel and compared to the present data only, given that this study is the first investigating di-n-propyl ether oxidation.

Experimental approach

Experiments were carried out in a fused silica jet-stirred reactor settled inside a stainless-steel pressure resistant jacket. An electrical oven enabled to perform experiments up to c.a. 1280K. The temperature within the reactor was continuously monitored by a Pt/Pt-Rh thermocouple located inside a thin wall fused silica tube to prevent catalytic reactions on the metallic wires.

Initial fuel mole fraction was 1000 ppm for all experiments, pressure and residence time (τ) were held constant 10 atm and 0.7s. The reactive mixtures were highly diluted by nitrogen to avoid high heat release inside the reactor and experiments were performed at temperatures ranging from 450 to 1160 K similar to our previous studies [6, 9]. The liquid fuel was atomized by a nitrogen flow and vaporized through a heated chamber. Reactants were brought separately to the reactor to avoid premature reactions and then injected by 4 injectors providing stirring. Flow rates of the diluent and reactants were controlled by mass flowmeters. A low-pressure sonic probe was used to freeze the reactions and take samples of the reacting mixtures.

Online analyses were performed after sending the samples via a heated line to a Fourier transform infrared (FTIR) spectrometer for the quantification of H_2O, CO, CO_2, and CH_2O. Samples were also stored at ca. 40 mbar in Pyrex bulbs for further analyses using gas chromatography (GC). Two gas chromatographs with a flame ionization detector (FID) were used: one equipped with a DB624 column to quantify oxygenated compounds and the other one with a CP-Al_2O_3/KCl column to quantify hydrocarbons. Identification of the products was done by GC/MS on a Shimadzu GC2010 Plus, with electron impact (70 eV) as the ionization mode. Hydrogen profiles were measured using a GC-TCD (thermal conductivity detector) equipped with a CP-CarboPLOT P7 column. The species quantified in this study include di-n-propyl-ether (DPE), H_2, H_2O, CO, CO_2, C_2H_4, CH_4, C_2H_6, C_3H_6, formaldehyde, propanal, acetaldehyde, and propanoic acid. Some other minor oxygenated species were also identified, such as 2-ethyl-4-methyl-1,3-dioxolane, 2-(propoxymethyl)oxirane, and traces of propyl formate and ethyl formate. The cyclic ethers cited are proper to DPE low-temperature chemistry, and they are formed in trace amounts. A quantification is therefore not done, also including the fact that these species were not directly calibrated and that we did not prefer to use an effective carbon method for molar fractions of few ppm. The carbon balance was checked for each sample and was found to be typically within ±10–15%.

Kinetic modeling

As the study of DPE is in line with our previous studies on diethyl ether (DEE) and di-n-butyl ether (DBE), a sub-mechanism was developed in a similar way to those of DEE and DBE and integrated into the mechanism as provided in [6]. In the present DPE sub-mechanism, rate constants of the main reactions were adopted from the literature, as follows:

- Reactions of hydrogen abstraction from fuel by OH radicals are taken from Zhou et al. [10] for the alpha C–H site. For the beta C–H site, the rate constant is evaluated by fitting to the theoretical calculations performed by [11-13] for the beta C–H in n-butanol. For the gamma C–H site, the rate constant is also assigned by fitting to the calculations of [11-13] and the measurements of Droege and Tully [14] for the delta C–H bond in n-butanol, as this one is the further away from the alcoholic carbon.

- Reactions of hydrogen abstraction from fuel by H atoms are taken from the theoretical study of Ogura et al. [15] for the alpha site. For the beta and gamma C–H bonds, rate constants are adopted from Tsang [16].

- H-abstraction rate constants by HO_2 and CH_3 radicals are adopted from the theoretical studies of Mendes et al. [17] and Xu et al. [18], respectively.

- Rate constants for $R+O_2 \rightleftharpoons RO_2$ reactions are adopted from Goldsmith et al. [19], both for 1st and 2nd addition.

- Rate constants for $RO_2 \rightleftharpoons$ QOOH, QOOH $\rightleftharpoons$ cyclic ether + OH are adopted from Villano et al. [20, 21].

- Beta-scission reactions of fuel radicals and those of QOOH radicals are adopted from the theoretical calculations of Villano et al. [21], Sakai et al. [22], and from our previous calculations on DBE [9].

- Other reactions related to low-temperature chemistry are taken analogous to our previous DBE model [9].

- Unimolecular decomposition reactions of DPE were taken from the study of Yasunaga et al. [1] in analogy with DEE. These reactions have no importance under present experimental conditions.

Thermochemistry of the fuel, fuel radical as well as all related low-temperature species were calculated using Thergas [23] which uses group additivity methods as proposed by Benson [24]. The JSR simulations were carried out with the Perfectly Stirred Reactor (PSR) code of Chemkin II package [25]. Results are shown in the following figures.

Results and discussion

Fuel conversion and fuel mole fractions for all experiments are presented in Figure 1.

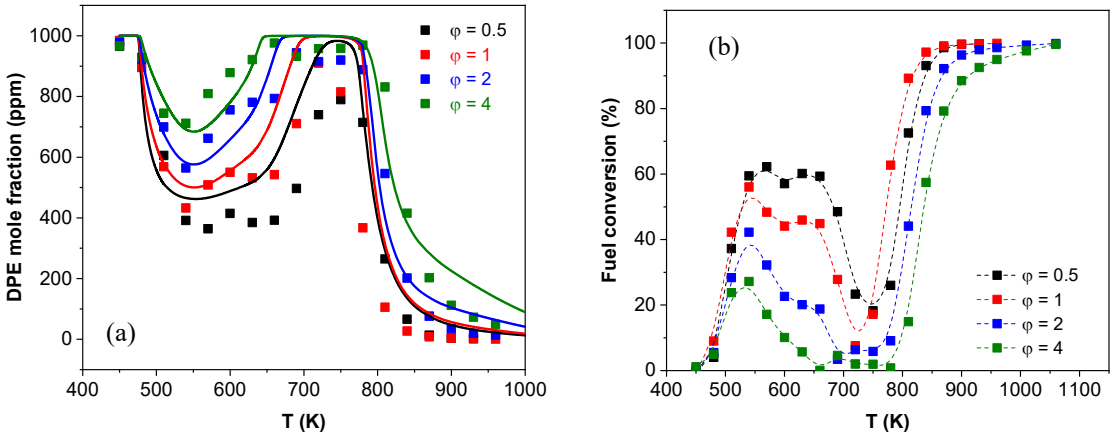

Figure 1. DPE mole fraction profiles (a) and conversion (b) for all mixtures

DPE shows a strongly pronounced low-temperature reactivity, followed by an NTC region (Figure 1a). For example, the NTC region for the φ = 1 and 2 mixtures, begin around 530 K and arrive to a plateau around 600 K. Then within a temperature window of ~ 60 K, no further fuel conversion is observed, and past 660 K reactivity decreases again. This behavior resembles what was previously observed in DBE oxidation as double-NTC [9], better demonstrated in Figure 1b. For the φ = 0.5 mixture, it would not be adequate to reach this conclusion as the single experimental point (600 K) that could prove this behavior is within experimental uncertainty. On the other hand, the φ = 4 mixture does not show this behavior, also the temperature zone between the end of NTC and start of high-temperature reactivity is wider for this mixture, and approaches zero between 660–780 K.

The kinetic model can predict the NTC behavior except for the "2nd NTC" region, although a small difference in the slope can be observed for the lean mixture. These kinetic uncertainties are due to the rate constants adopted in the low-temperature oxidation mechanism. Often, these rate constants are more adequate for alkane oxidation and analogies have to be made in developing mechanisms for oxygenated compounds. The effect of some of these rate constants will be illustrated in the coming sections.

In the following figures (2–5), experimental results are presented along with simulations, a representative 15% uncertainty bar is added to the fuel profile. General

tendency is well predicted by the model, some discrepancies exist due to the chosen rate constants in low-temperature oxidation sub-mechanism. From Figure 1, one can speculate that the model slightly under-predicts the experimental reactivity of the φ = 0.5 and 1 mixtures in the NTC region.

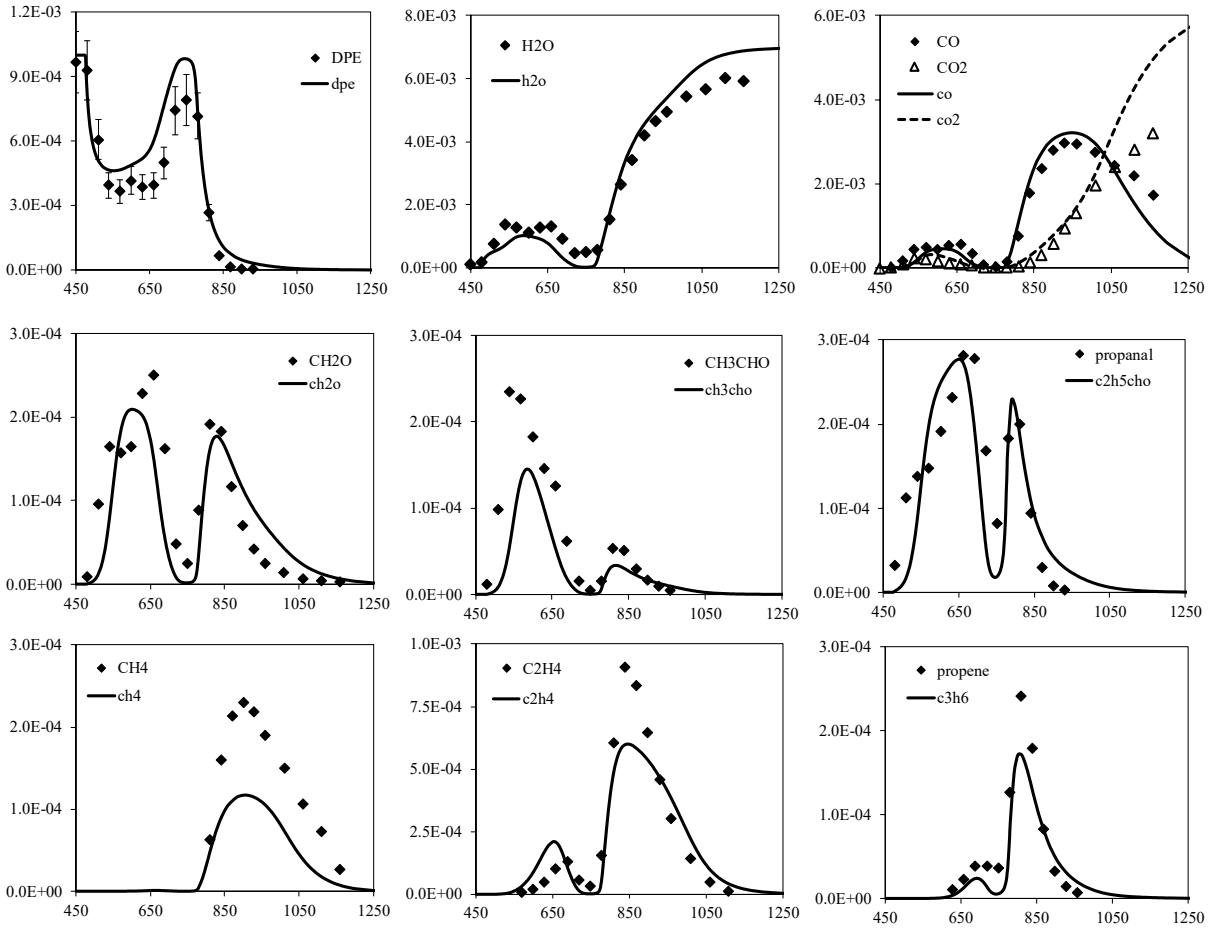

Figure 2. Mole fraction profiles as a function of reactor temperature (φ = 0.5)

The most important low-temperature products observed were formaldehyde, propanal, acetaldehyde and propanoic acid. Formaldehyde is a typical marker of low-temperature reactivity of many fuels and is formed in large amounts in DPE oxidation as well. The typical oxygenated intermediate in the case of DPE is propanal. Similarly, butanal and acetaldehyde were observed in large quantities in DBE and DEE oxidation, respectively.

An interesting feature of ether oxidation turns out to be the formation of carboxylic acids. As an example, formic acid was identified and quantified in earlier studies by Curran et al. [26] in a flow reactor and by Dagaut et al. [27] in a jet-stirred reactor and more recently by Moshammer et al. [28] in a jet-stirred reactor and by Wang et al. [29] in a flow reactor study. In contrast to these studies, in their jet-stirred reactor study on low-temperature DME oxidation by Rodriguez et al. [30], no formation of formic acid was reported.

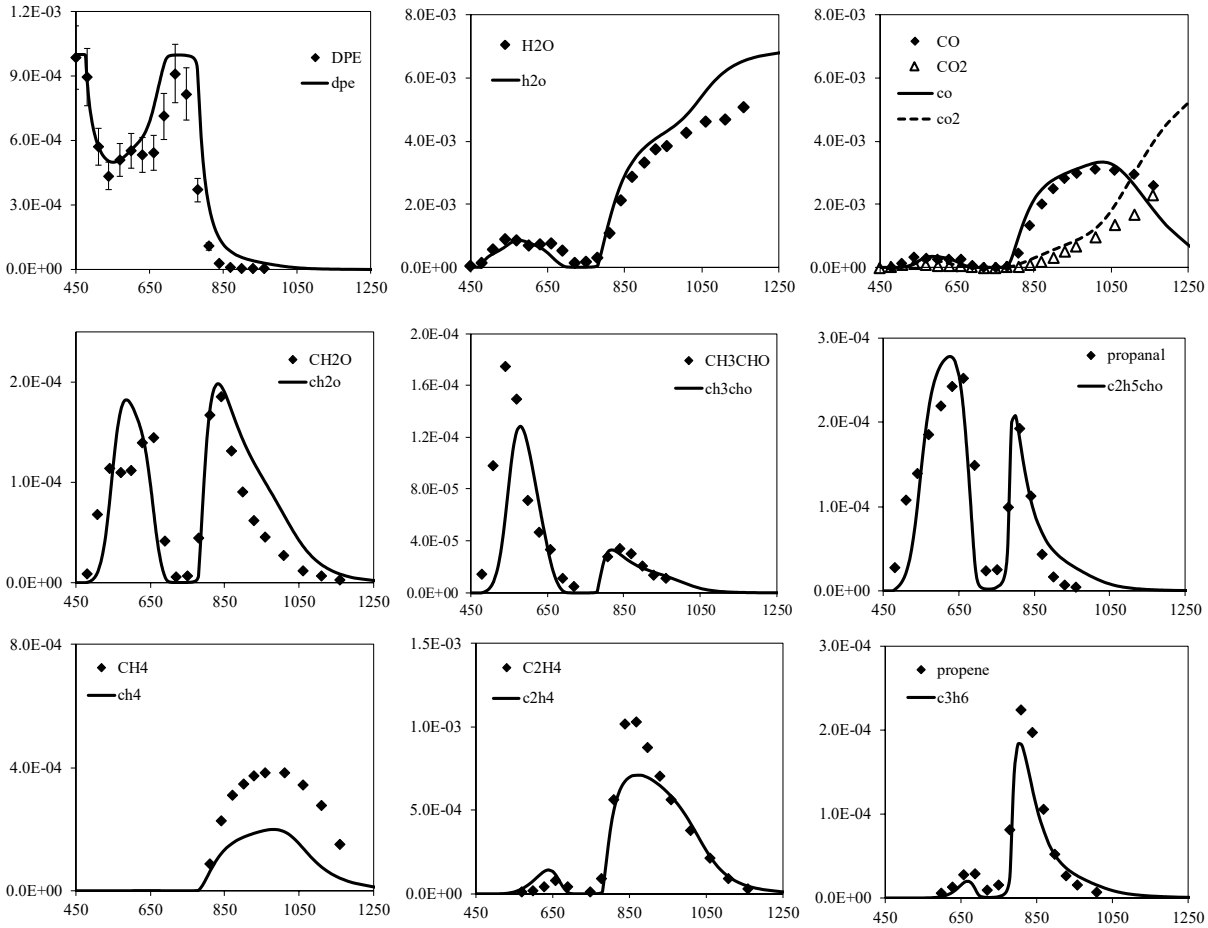

Figure 3. Mole fraction profiles as a function of reactor temperature (φ = 1)

In our DEE study, acetic acid was quantified at low temperatures in considerable quantities and in DBE oxidation butanoic acid was identified for some experiments but not quantified. The formation routes of these acids are unclear and probably due to an unconventional pathway followed by the radicals formed by ketohydroperoxide decomposition. Formation of propanoic acid cannot be explained by analogy to the formic acid formation pathway first proposed by Curran [26] and later calculated by Wang and co-workers [29]. This formic acid pathway involves an internal hydrogen transfer from the acyl site of the $^{\bullet}OCH_2OCHO$ radical (formed by C–O scission of the aldohydroperoxide) followed by its α-scission to formic acid and CO. However, in DPE oxidation the most abundant carbonylhydroperoxide is a ketohydroperoxide (shown in Fig 7 as c3oc31ohhket1) hence such a pathway is not possible. Therefore, although propanoic acid is quantified with a 125 ppm peak for φ = 0.5 mixture and 16 ppm peak for φ = 4 mixture, its profile is not simulated.

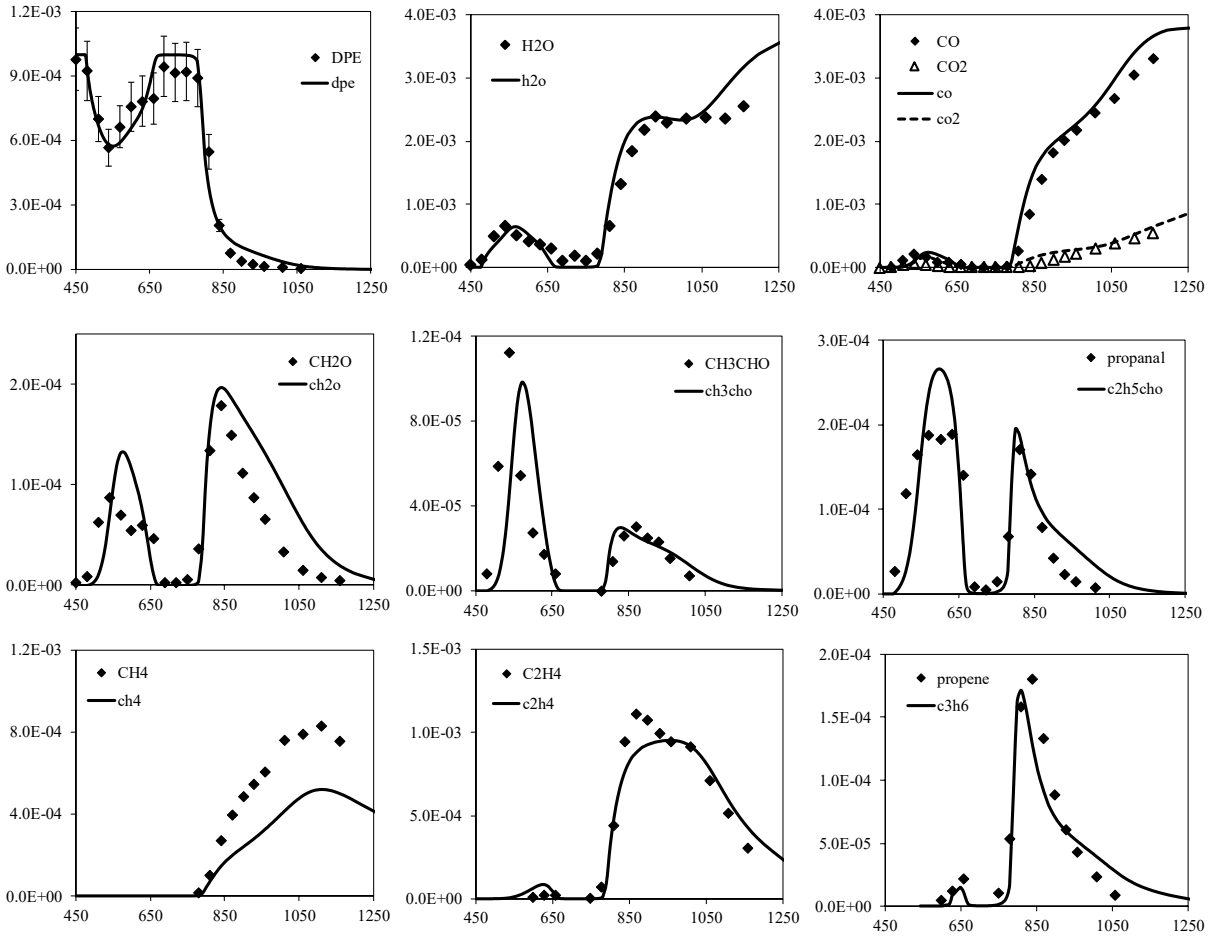

Figure 4. Mole fraction profiles as a function of reactor temperature (φ = 2)

Generally speaking, for all conditions, kinetic model agrees reasonably well with the data. A factor of 1.5–2 discrepancy is observed with ethylene peak value and CO is slightly over-predicted in rich mixtures.

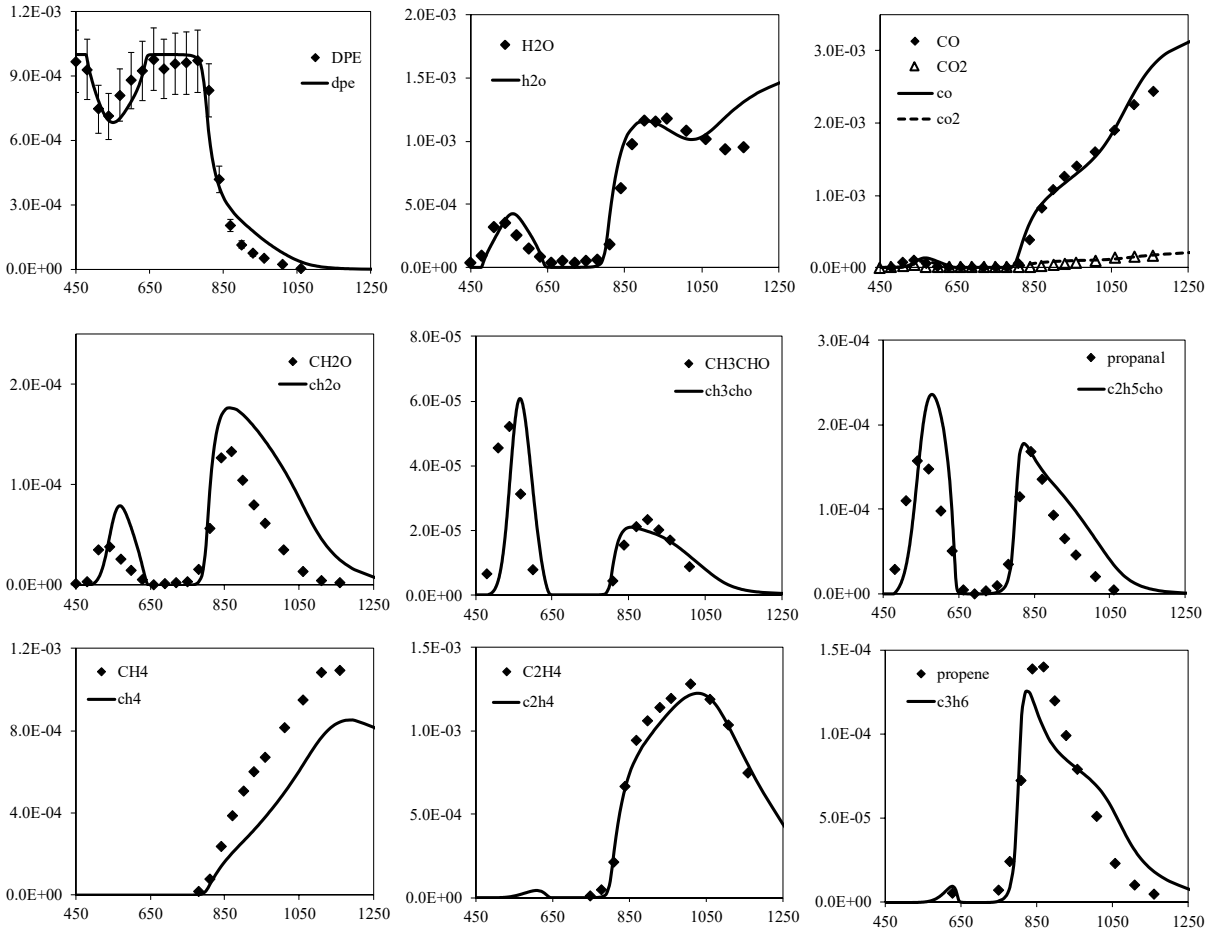

Figure 5. Mole fraction profiles as a function of reactor temperature (φ = 4)

Reaction pathways

DPE can form three distinct fuel radicals, α-radical (dpe1), β- (dpe2) and γ- (dpe3) radicals. C–H bond dissociation energies for DPE are calculated on G3B3 and CBS-QB3 levels using Gaussian09 [31] and are presented below. According to this, the alpha C–H bond is the weakest and therefore the dpe1 radical is favored, which was naturally the case with DBE and DEE. Also, note that the gamma C–H bond energy is similar to a primary C–H bond in alkane, confirming the choice of analogy.

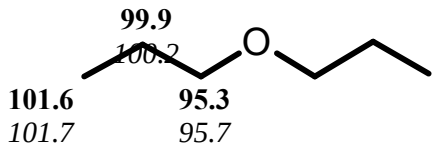

Figure 6. C–H bond dissociation energies of DPE calculated with G3B3 (bold) and CBS-QB3 (italic)

Main reaction pathways are presented in Figure 7 for the low-temperature oxidation of DPE, which is mainly consumed by H-abstraction reactions by OH radicals and this is the case at any temperature. The percentages are evaluated at 500 K for the φ = 1 mixture, as an example.

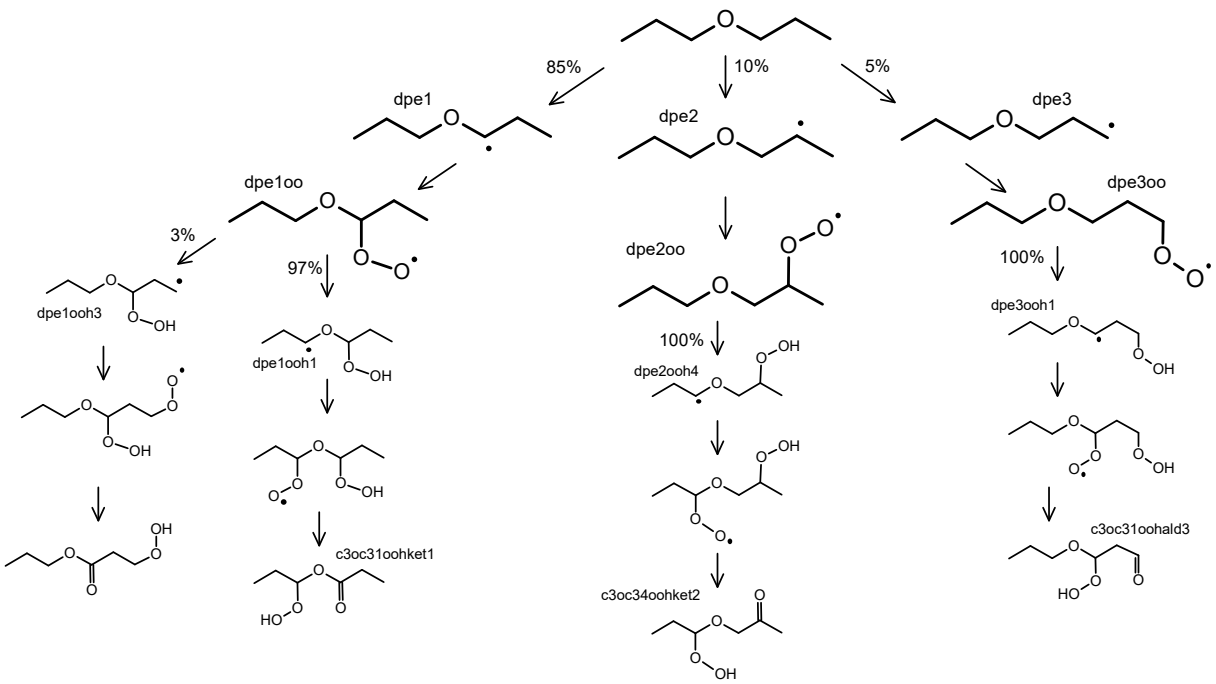

Figure 7. Main reaction pathways at low temperatures (% are given at 500 K, φ = 1)

At low temperatures, addition of fuel radicals to molecular oxygen is dominant forming the RO_2 radicals. The RO_2 radicals can go through isomerization (internal hydrogen transfer) to form QOOH radicals. At these conditions the QOOH produced via 6-membered transition states are favored and lead to the species and pathways as presented below. Propanal formation at low temperature is via ketohydroperoxide decomposition, which is probably the most important in low-temperature chemistry. In fact, this reaction is often written in one step with chain branching fragments and an OH radical as products. The rate constant used for this reaction in various mechanisms comes from an experimental study by Sahetchian et al. [32] focusing on the decomposition of organic hydroperoxides, and it can be approximately written as $k = 1x10^{16}\ exp\ (-43\ kcal/RT)$. A slightly different pre-exponential factor or activation energy can be found in various literature mechanisms.

The Figure 8 shows the effect of this rate constant on the predictions of fuel mole fraction. Activation energy of the KHP decomposition was modified by up to 6 kcal/mol. This very low activation energy was proposed in the kinetic model of Cai et al. [33] on DBE oxidation for all KHPs possible. The considerable effect of this rate constant on mole fraction profiles can be clearly observed. We have also included the theoretical study of Goldsmith et al. [34] on the decomposition of $HOOCH_2CH_2CHO$, via various channels. This rate constant appears to be very close to the one obtained by reducing the original activation energy by 3 kcal, i.e. when using $1x10^{16}\ exp\ (-40\ kcal/RT)$ as the rate constant, which is therefore adopted here. Furthermore, in order to highlight the effect of $R + O_2 \rightleftharpoons RO_2$ rate constant, we have compared predictions with two theoretically calculated rate constants by Goldsmith [19] and Miyoshi [35], both are widely used in kinetic mechanisms. Actually, this reversible reaction is very sensitive to thermochemistry and note that in this study, group additivity is used. Also, as is the case with the rate constants adopted from Villano et al. [20, 21] for this reaction class, very often these calculations are done for alkanes. The similarities assumed are therefore done compared to alkanes although the fuel is an ether. This probably adds an additional uncertainty to the predictions.

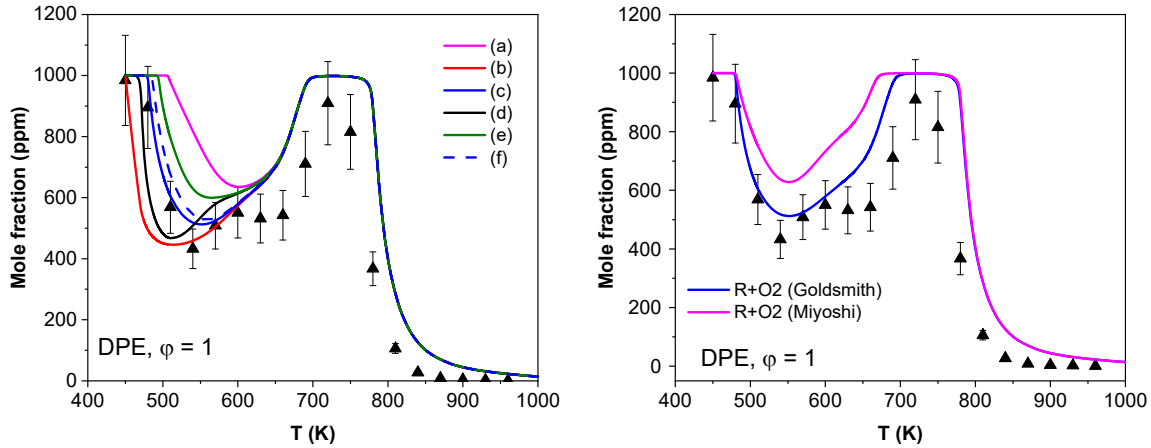

Figure 8. Effect of KHP decomposition (left) and R + O_2 ⇌ RO_2 (right) reactions on model predictions. For the figure on the left : (a) assuming E_a = 43 kcal/mol for all KHP, (b) assuming E_a = 37 kcal/mol for all KHP, (c) assuming E_a = 40 kcal/mol for all KHP, (d) assuming Ea = 37 kcal/mol except for c3oc31oohket1, (e) assuming Ea = 40 kcal/mol except for c3oc31oohket1, (f) using the rate constant calculated by Goldsmith et al. [34] for the reaction $HOOCH_2CH_2CHO \rightarrow {}^{\bullet}OCH_2CH_2CHO + {}^{\bullet}OH$.

Comparison of DEE, DPE and DBE

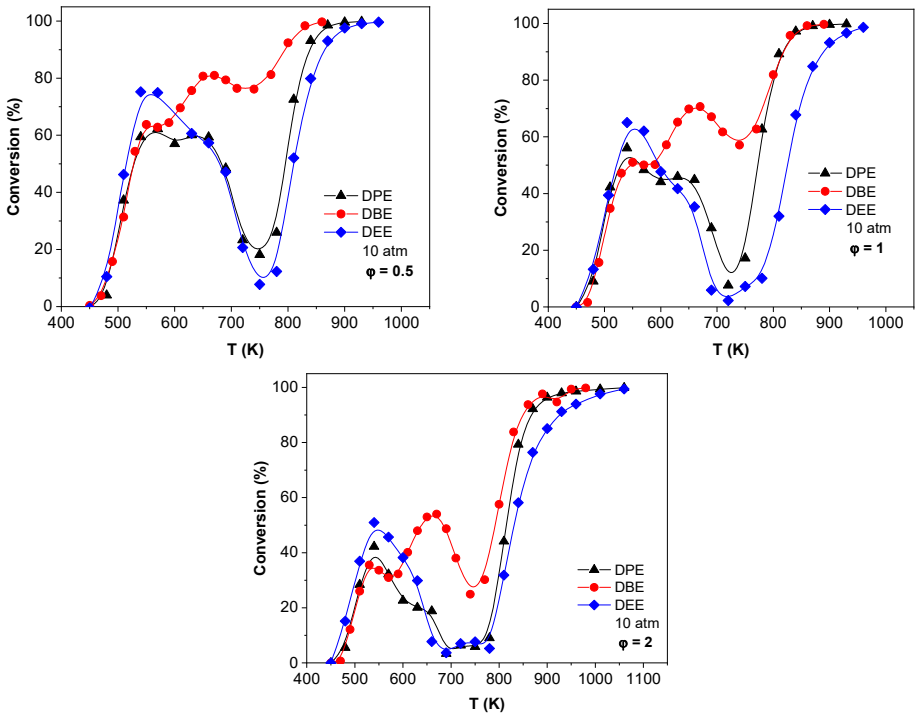

Figure 9. Comparison of the reactivity of DEE, DPE and DBE, all studied under same conditions (lines added to guide the eye)

Figure 9 illustrates the experimental fuel conversion of DEE, DPE and DBE, in order to compare their relative reactivity. On this plot one can clearly see the differences and similarities. All three ethers are very reactive, conversion begins right above 450 K, and they all exhibit a strong low-temperature reactivity and NTC behavior. On the other hand, DBE shows a clear double-NTC behavior, which is less pronounced in DPE oxidation and appears

to be absent in the case of DEE. Among the three, DBE stands out with its very high conversion even in both NTC regions. For example, including the NTC region, DBE conversion is always higher than 60% for φ = 0.5 mixture.
The particularity in DBE oxidation stems from the fact that even at these low temperatures, owing to its long chain, formation of small radicals is possible. Its oxidation can produce radicals such as n-propyl, mostly from the ketohydroperoxide $C_3H_7C(=O)OCH(OOH)C_3H_7$ decomposition. Decomposition of this ketohydroperoxide also produces butanal, which gives n-propyl radicals by alpha-scission of its acyl radical at the low-intermediate temperature range, and n-butyl radicals at intermediate temperatures. Therefore the low-intermediate temperature regime in DBE oxidation is also controlled by the pathways followed by smaller radicals that have their own low-temperature reactivity. On the other hand in DEE oxidation, the chain is two carbon atoms smaller and these interactions do not take place. DPE, however, is in midway between DEE and DBE and produces ethyl radicals in abundance during its oxidation. Ethyl radicals add to molecular oxygen at lower temperatures and follow rather dismutation pathways (producing ethanol, for example). They do not trigger an NTC type of chemistry of their own like in DBE however they are more reactive than the methyl radicals in DEE oxidation. Note that these observations hold for the investigated conditions of 1000 ppm initial fuel mole fraction, 10 atm and for a residence time of 700 ms and that at other conditions reactivity profiles may be different. More details on DBE and DEE oxidation can be found in the corresponding papers [6, 9].
At these temperatures thermochemistry is of crucial importance, hence the thermochemical values (especially RO_2, QOOH, OOQOOH) have to be as accurate as possible in addition to the kinetics. Group additivity method may have its limits with such complex radicals. More kinetic data is certainly useful for our understanding of the detailed chemistry, however we should not neglect the effect of the uncertainties in thermochemistry, which are high with such large and complex radicals.

Summary

In line with our previous studies on the oxidation of ethers, in the present work high-pressure oxidation of di-n-propyl ether was studied in a jet-stirred reactor at various equivalence ratios (φ = 0.5–4), for the first time. DPE exhibited an important low-temperature reactivity and a double-NTC behavior, although to a lesser extent that that of DBE. A kinetic model was developed in order to understand the oxidation patterns based on our previous efforts and literature. This model shows a good agreement in general, however some discrepancies arise from uncertainties in the rate parameters used. In order to extend this study to atmospheric pressure, more experiments will be performed. Also, theoretical calculations could be useful in interpreting the low-temperature oxidation behavior of the ether-related species.

Acknowledgements

Authors gratefully acknowledge funding received from Labex Caprysses (convention ANR-11-LABX-0006-01).

References

[1] Yasunaga K, Gillespie F, Simmie JM, Curran HJ, Kuraguchi Y, Hoshikawa H, et al. A Multiple Shock Tube and Chemical Kinetic Modeling Study of Diethyl Ether Pyrolysis and Oxidation. The Journal of Physical Chemistry A 2010;114(34):9098-109.

[2] Gillespie F, Metcalfe WK, Dirrenberger P, Herbinet O, Glaude P-A, Battin-Leclerc F, et al. Measurements of flat-flame velocities of diethyl ether in air. Energy 2012;43(1):140-5.
[3] Werler M, Cancino LR, Schiessl R, Maas U, Schulz C, Fikri M. Ignition delay times of diethyl ether measured in a high-pressure shock tube and a rapid compression machine. Proceedings of the Combustion Institute 2015;35(1):259-66.
[4] Vin N, Herbinet O, Battin-Leclerc F. Diethyl ether pyrolysis study in a jet-stirred reactor. Journal of Analytical and Applied Pyrolysis 2016;121:173-6.
[5] Tran L-S, Pieper J, Carstensen H-H, Zhao H, Graf I, Ju Y, et al. Experimental and kinetic modeling study of diethyl ether flames. Proceedings of the Combustion Institute 2017;36(1):1165-73.
[6] Serinyel Z, Lailliau M, Thion S, Dayma G, Dagaut P. An experimental chemical kinetic study of the oxidation of diethyl ether in a jet-stirred reactor and comprehensive modeling. Combustion and Flame 2018;193:453-62.
[7] Uygun Y. Ignition studies of undiluted diethyl ether in a high-pressure shock tube. Combustion and Flame 2018;194:396-409.
[8] Tran L-S, Herbinet O, Li Y, Wullenkord J, Zeng M, Bräuer E, et al. Low-temperature gas-phase oxidation of diethyl ether: Fuel reactivity and fuel-specific products. Proceedings of the Combustion Institute 2019;37(1):511-9.
[9] Thion S, Togbé C, Serinyel Z, Dayma G, Dagaut P. A chemical kinetic study of the oxidation of dibutyl-ether in a jet-stirred reactor. Combustion and Flame 2017;185:4-15.
[10] Zhou C-W, Simmie JM, Curran HJ. An ab initio/Rice-Ramsperger-Kassel-Marcus study of the hydrogen-abstraction reactions of methyl ethers, H3COCH3-x(CH3)x, x = 0-2, by [radical dot]OH; mechanism and kinetics. Physical Chemistry Chemical Physics 2010;12(26):7221-33.
[11] Zhou C-W, Simmie JM, Curran HJ. Rate constants for hydrogen-abstraction by OH from n-butanol. Combustion and Flame 2011;158(4):726-31.
[12] Zádor J, Miller JA. Hydrogen Abstraction From N-, I-Propanol And Nbutanol: A Systematic Theoretical Approach. *7th US National Techical Meeting, Combust. Inst.* Atlanta, USA: Combust. Inst.; 2011:483-8
[13] Seal P, Oyedepo G, Truhlar DG. Kinetics of the Hydrogen Atom Abstraction Reactions from 1-Butanol by Hydroxyl Radical: Theory Matches Experiment and More. The Journal of Physical Chemistry A 2013;117(2):275-82.
[14] Droege AT, Tully FP. Hydrogen atom abstraction from alkanes by hydroxyl. 5. n-Butane. The Journal of Physical Chemistry 1986;90(22):5937-41.
[15] Ogura T, Miyoshi A, Koshi M. Rate coefficients of H-atom abstraction from ethers and isomerization of alkoxyalkylperoxy radicals. Physical Chemistry Chemical Physics 2007;9(37):5133-42.
[16] Tsang W. Chemical Kinetic Data Base for Combustion Chemistry. Part 3: Propane. Journal of Physical and Chemical Reference Data 1988;17(2):887-951.
[17] Mendes J, Zhou C-W, Curran HJ. Rate Constant Calculations of H-Atom Abstraction Reactions from Ethers by HȮ2 Radicals. The Journal of Physical Chemistry A 2014;118(8):1300-8.
[18] Xu ZF, Park J, Lin MC. Thermal decomposition of ethanol. III. A computational study of the kinetics and mechanism for the CH3+C2H5OH reaction. The Journal of Chemical Physics 2004;120(14):6593-9.
[19] Goldsmith CF, Green WH, Klippenstein SJ. Role of O2 + QOOH in Low-Temperature Ignition of Propane. 1. Temperature and Pressure Dependent Rate Coefficients. The Journal of Physical Chemistry A 2012;116(13):3325-46.

[20] Villano SM, Huynh LK, Carstensen H-H, Dean AM. High-Pressure Rate Rules for Alkyl + O2 Reactions. 1. The Dissociation, Concerted Elimination, and Isomerization Channels of the Alkyl Peroxy Radical. The Journal of Physical Chemistry A 2011;115(46):13425-42.
[21] Villano SM, Huynh LK, Carstensen H-H, Dean AM. High-Pressure Rate Rules for Alkyl + O2 Reactions. 2. The Isomerization, Cyclic Ether Formation, and β-Scission Reactions of Hydroperoxy Alkyl Radicals. The Journal of Physical Chemistry A 2012;116(21):5068-89.
[22] Sakai Y, Ando H, Chakravarty HK, Pitsch H, Fernandes RX. A computational study on the kinetics of unimolecular reactions of ethoxyethylperoxy radicals employing CTST and VTST. Proceedings of the Combustion Institute 2015;35(1):161-9.
[23] Muller C, Michel V, Scacchi G, Côme GM. Thergas - A computer program for the evaluation of thermochemical data of molecules and free radicals in the gas phase. Journal de chimie physique et de physico-chimie biologique 1995;92(5):1154-78.
[24] Benson SW. Thermochemical Kinetics. New York: Wiley; 1976.
[25] Glarborg P, Kee RJ, Grcar JF, Miller JA. PSR: A Fortran Program for Modeling Well-Stirred Reactors, Report No. SAND86-8209, Sandia National Laboratories, Albequerque, NM. 1986.
[26] Curran HJ, Fischer SL, Dryer FL. The reaction kinetics of dimethyl ether. II: Low-temperature oxidation in flow reactors. International Journal of Chemical Kinetics 2000;32(12):741-59.
[27] Dagaut P, Luche J, Cathonnet M. The Low Temperature Oxidation of DME and Mutual Sensitization of the Oxidation of DME and Nitric Oxide: Experimental and Detailed Kinetic Modeling. Combustion Science and Technology 2001;165(1):61-84.
[28] Moshammer K, Jasper AW, Popolan-Vaida DM, Lucassen A, Diévart P, Selim H, et al. Detection and Identification of the Keto-Hydroperoxide (HOOCH2OCHO) and Other Intermediates during Low-Temperature Oxidation of Dimethyl Ether. The Journal of Physical Chemistry A 2015.
[29] Wang Z, Zhang X, Xing L, Zhang L, Herrmann F, Moshammer K, et al. Experimental and kinetic modeling study of the low- and intermediate-temperature oxidation of dimethyl ether. Combustion and Flame 2015;162(4):1113-25.
[30] Rodriguez A, Frottier O, Herbinet O, Fournet R, Bounaceur R, Fittschen C, et al. Experimental and Modeling Investigation of the Low-Temperature Oxidation of Dimethyl Ether. The Journal of Physical Chemistry A 2015;119(28):7905-23.
[31] Frisch MJT, G. W.; Schlegel, H. B.; Scuseria, G. E.; Robb, M. A.; Cheeseman, J. R.; Scalmani, G.; Barone, V.; Mennucci, B.; Petersson, G. A.; Nakatsuji, H.; Caricato, M.; Li, X.; Hratchian, H. P.; Izmaylov, A. F.; Bloino, J.; Zheng, G.; Sonnenberg, J. L.; Hada, M.; Ehara, M.; Toyota, K.; Fukuda, R.; Hasegawa, J.; Ishida, M.; Nakajima, T.; Honda, Y.; Kitao, O.; Nakai, H.; Vreven, T.; Montgomery, J. A., Jr. ; Peralta, J. E.; Ogliaro, F.; Bearpark, M.; Heyd, J. J.; Brothers, E.; Kudin, K. N.; Staroverov, V. N.; Kobayashi, R.; Normand, J.; Raghavachari, K.; Rendell, A.; Burant, J. C.; Iyengar, S. S.; Tomasi, J.; Cossi, M.; Rega, N.; Millam, N. J.; Klene, M.; Knox, J. E.; Cross, J. B.; Bakken, V.; Adamo, C.; Jaramillo, J.; Gomperts, R.; Stratmann, R. E.; Yazyev, O.; Austin, A. J.; Cammi, R.; Pomelli, C.; Ochterski, J. W.; Martin, R. L.; Morokuma, K.; Zakrzewski, V. G.; Voth, G. A.; Salvador, P.; Dannenberg, J. J.; Dapprich, S.; Daniels, A. D.; Farkas, Ö.; Foresman, J. B.; Ortiz, J. V.; Cioslowski, J.; Fox, D. J. Gaussian 09, Revision D.01. Wallingford CT: Gaussian, Inc.; 2009.
[32] Sahetchian KA, Rigny R, Tardieu de Maleissye J, Batt L, Anwar Khan M, Mathews S. The pyrolysis of organic hydroperoxides (ROOH). Symposium (International) on Combustion 1992;24(1):637-43.

[33] Cai L, Sudholt A, Lee DJ, Egolfopoulos FN, Pitsch H, Westbrook CK, et al. Chemical kinetic study of a novel lignocellulosic biofuel: Di-n-butyl ether oxidation in a laminar flow reactor and flames. Combustion and Flame 2014;161(3):798-809.
[34] Goldsmith CF, Burke MP, Georgievskii Y, Klippenstein SJ. Effect of non-thermal product energy distributions on ketohydroperoxide decomposition kinetics. Proceedings of the Combustion Institute 2015;35(1):283-90.
[35] Miyoshi A. Systematic Computational Study on the Unimolecular Reactions of Alkylperoxy (RO2), Hydroperoxyalkyl (QOOH), and Hydroperoxyalkylperoxy (O2QOOH) Radicals. The Journal of Physical Chemistry A 2011;115(15):3301-25.